

# Enhanced Performance of an All-Vanadium Redox Flow Battery Employing Graphene Modified Carbon Paper Electrodes

Barun Chakrabarti, Dan Nir, Vladimir Yufit, P. V. Aravind, Nigel Brandon

**Abstract**—Fuel cell grade gas-diffusion layer carbon paper (CP) electrodes are subjected to electrophoresis in  $N,N'$ -dimethylformamide (DMF) consisting of reduced graphene oxide (rGO). The rGO modified electrodes are compared with CP in a single asymmetric all-vanadium redox battery system (employing a double serpentine flow channel for each half-cell). Peak power densities improved by 4% when the rGO deposits were facing the ion-exchange membrane (cell performance was poorer when the rGO was facing the flow field). Cycling of the cells showed least degradation of the CP electrodes that were coated with rGO in comparison to pristine samples.

**Keywords**—All-vanadium redox flow batteries, carbon paper electrodes, electrophoretic deposition, reduced graphene oxide.

## I. INTRODUCTION

REDOX flow batteries are undergoing significant research activities in order to enhance their power densities and lifetimes whilst reducing their operating costs [1]-[3]. Since this decade, research led by the University of Tennessee has been focused on a zero-gap membrane electrode assembly that was inspired from the concept of the direct methanol fuel cell [4], [5].

The all-vanadium redox flow battery (VRFB) has been the main focus of such investigations [5]. CP electrodes sandwiching a Nafion 117 membrane has commonly been employed, but surprisingly the highest power density for a VRFB was reported using graphite felts [6]. Hence, recent investigations have focused on modifying the CPs to make them not only hydrophilic but also conductive to enhance the power densities [3]. For instance, thermal pre-treatment and stacking of several CP layers resulted in improved performances [7]. In addition, deposition of carbon nanoparticles on CP electrodes also resulted in about 8% enhancement of peak power densities [8]. Considering this fact, a consideration on how CPs would perform when sputtered with reduced graphene oxide (rGO) appears to be limited in the available literature [9].

In this work, an electrophoretic deposition (EPD) technique is utilized to coat rGO onto CP substrates in an effective manner [10]. The modified electrodes are then used to conduct polarization tests on VRFBs followed by redox cycling. Enhancements in power densities and cycling efficiencies are reported thereafter.

Barun Chakrabarti is with the Imperial College London, United Kingdom (e-mail: b.chakrabarti@imperial.ac.uk).

## II. EXPERIMENTAL

### A. Materials

The CP electrodes (GDL 10 AA Series Gas Diffusion Layer) were sourced from SGL Carbon Ltd. rGO was purchased from ACS Material (USA) and used as received. DMF, sulfuric acid (95% pure) and vanadium sulfate (99.9% metals basis) were purchased from VWR International (AnalaR NORMAPUR grade).

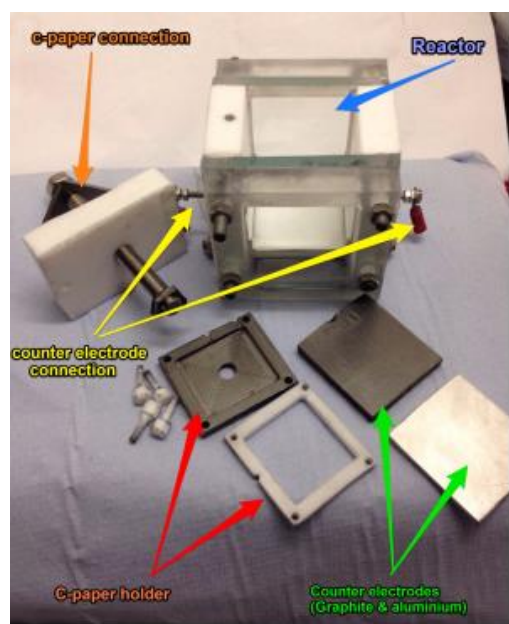
### B. EPD Reactor and Process

Due to the use of corrosive organic chemicals, the reactor was made of glass and graphite plates so that it was possible to observe the EPD process during experimental runs. A digital photo of the cylindrical EPD reactor is shown in Fig. 1 (a). The reactor was designed with Solid Works and made with a CNC machine as detailed in an earlier publication [11]. Horizontal EPD was performed as this was found to result in more uniform depositions [12].

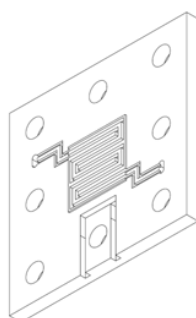
During EPD, a potential of 300 V was applied by means of a high voltage power supply (EA Elektro-Automatik, EA-PS 9750-04 2U). 0.1 g/L of rGO was ultrasonically dispersed in DMF for about 2h as reported in the literature [12]. CP (rinsed thoroughly with acetone and dried) was used as the working electrode (upper part of the reactor) whilst a graphite plate functioned as the counter (lower part). 15 mm inter-electrode distance was used to enhance deposition morphology. The reason for this was to allow uniform deposition as reported elsewhere [11].

### C. VRFB Details

The VRFB reactor was a single cell with two graphite current collector plates, each with a double serpentine flow field (designed in-house as shown in Fig. 1 (b)). CP electrodes with 410  $\mu\text{m}$  nominal thickness and 5  $\text{cm}^2$  active areas were used. Viton rubber gaskets (DuPont, thickness 0.4 mm) were used between the components to prevent electrolyte leakage and to limit the compression of the electrode to about 4 Nm in order to reduce contact resistance within the cell. Nafion 117 (DuPont) was used as the ion exchange membrane (without pre-treatment) to separate the half-cells. The cell was connected to the electrolyte tanks using Masterflex<sup>®</sup> Viton tubing (Watson Marlow), and a single peristaltic pump with two heads (Cole Parmer) supplied electrolyte to the cell at a constant flow rate of 100 mL/min as recommended in the literature [13].



(a)



(b)

Fig. 1 (a) Digital image of the key parts of the EPD reactor used in this as well as in an earlier investigation [11]; (b) Double serpentine flow fields on graphite current collector for the in-house designed VRFB. Reproduced with permission from Wiley [11]

#### D. Charge/Discharge

The electrolyte used consisted of 1 mol/L  $\text{VOSO}_4$  + 5 mol/L  $\text{H}_2\text{SO}_4$  for charging purposes as detailed elsewhere [11]. The volumes of the negative and positive electrolytes were 50 mL and 100 mL, respectively in a similar manner to the literature [7]. A constant voltage step of 1.8 V was used to charge the VRFB (using a Metrohm Autolab potentiostat) to a cut-off current of 10 mA [4], [5].

After the initial charge, the catholyte volume was halved to leave equal volumes for both half-cells. Polarization curves were then measured as described below. In addition, charge/discharge cycling was carried out after initial discharge of the electrolytes to a cut-off voltage of 0.8 V [14]. About 20 cycles were performed using a cell having pristine CP samples and later with rGO modified CP electrodes.

#### E. Polarization

Polarization curves and impedance spectroscopy were measured galvanostatically with the same Metrohm Autolab potentiostat as detailed by Zawodzinski and co-workers [5]. All discharge polarisation commenced with the battery at an initial state of charge (SoC) of 100%. During each step of generating the polarization curves, discharging lasted for 5 s followed by constant voltage charging (1.8 V) to maintain a 100% state-of-charge (all performed at room temperature).

High frequency resistance (HFR) was determined in exactly the same manner as reported in the literature [5]. In short, HFR was recorded within a frequency range of 10 to 100 kHz using AC pulse of 10 mV amplitude. Areal specific resistance (ASR) was determined as a combination of the HFR and the electrode area of 5 cm<sup>2</sup>. The ASR enabled the correction of polarization curves for ohmic ( $iR$ ) losses at a given current density in a similar manner to Aaron et al. [5].

#### F. Instrumentations and Characterizations

Scanning electron microscopy (SEM) on the rGO modified CP sample was conducted using a JEOL JSM 6010 LA (USA) at 5 kV. Zeta potentials were measured using a Brookhaven PALS Zeta Potential Analyzer (version 3.48). rGO + DMF samples were diluted to 1/50 their original concentrations. All measurements were performed in triplicate at room temperature and pressure and the mean was estimated by the PALS Zeta Potential Analyzer software.

Raman spectra from four CP samples, shown in Table I, were recorded using a Renishaw 2000 CCD (charge-coupled device) spectrometer equipped with an Olympus BH-2 confocal microscope as detailed elsewhere [11]. All spectra shown here were collected using a 514-nm laser excitation source with power in the range of 0.5 – 5.0 mW at the focal point. Incident power levels were limited to a power density less than 0.1 mW/ $\mu\text{m}^2$ , to avoid laser damage of the surface [11]. Over 40 spectra were collected from random locations on each sample to ensure a statistically meaningful characterization.

TABLE I  
CP SAMPLES (UNTREATED AND TREATED) ANALYZED BY RAMAN SPECTROSCOPY. FOR THE DOUBLE-SIDED DEPOSITED SAMPLES; THE FIRST SIDE THAT UNDERWENT EPD IS CLASSIFIED AS THE "LIGHTER SIDE" WHEREAS THE SECOND SIDE IS LABELLED AS THE "DARKER SIDE"

Sample	Description
1	Untreated
2	Single-sided rGO deposit
3	Double-sided rGO deposit (lighter side)
4	Double-sided rGO deposit (darker side)

### III. RESULTS AND DISCUSSION

#### A. EPD

DMF was chosen as the solvent for EPD because the literature indicated that deposition was most uniform when compared to several other solvents [13], [15]. Zeta potential measurements showed that the rGO was positively charged, and thus, the working electrode was negative in polarity [11].

SEM images of rGO deposited on CP substrates are shown in Fig. 2. Fig. 2 (a) shows the untreated CP whereas Fig. 2 (b) shows the same substrate with rGO deposited at 300 V. The CP is highly porous and has a complex structure. Long spaghetti like carbon fibers are interwoven with one another and 'glued' together with carbon flakes. It is clear that the EPD process resulted in thick deposits of rGO and greater penetration within the fibers that changed the surface morphology of the CP. Such deposits were characterized as having amorphous structures by means of Raman spectroscopy (Fig. 2 (c)). A similar figure was also published elsewhere [11].

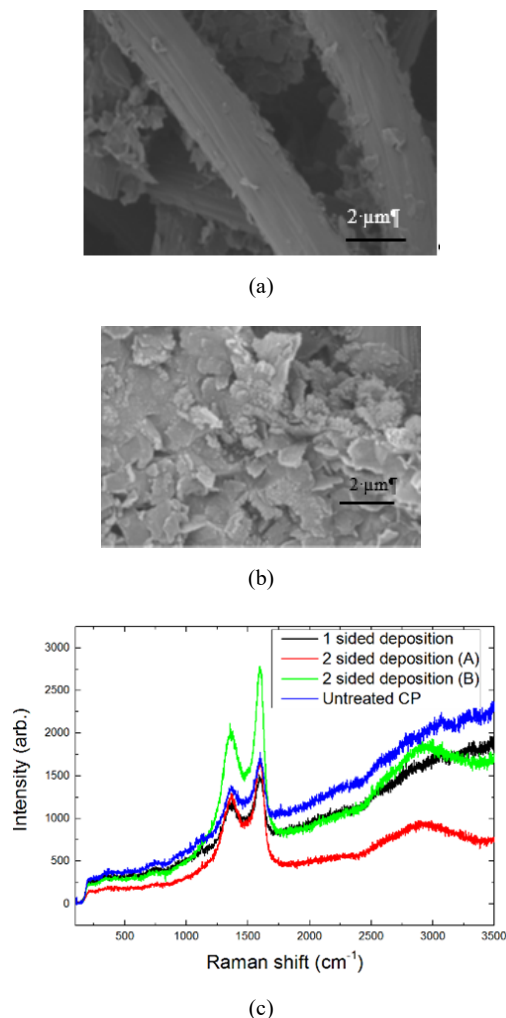


Fig. 2 (a) SEM image of CP without any deposition (untreated); (b) SEM image of CP with rGO deposited at 300 V (at the same corresponding magnification as the untreated sample); and (c) Normalized Raman responses relative to the G-peak, generated from 40+ spectra collected from untreated and treated CP samples whereby (A) refers to the rGO deposit on one side and (B) refers to deposition on the other side (actual 2-sided deposition). Reproduced with permission from Wiley [11]

### B. Polarization Results

Xu et al. [12] showed that low electrolyte flow rates of 100

mL/min or less resulted in better performance of VRFBs without any flow fields than otherwise. This may have been because turbulence ensures better coverage of the CP than a slow laminar flow when flow fields are employed. Therefore, in this research, the flow rate was fixed at 100 mL/min and not less.

Fig. 3 shows the polarization results for the VRFB operating with three different electrode configurations: (a) untreated CP; (b) rGO treated CP facing the flow fields; and (c) rGO treated CP facing the membrane. The highest limiting current and peak power densities are measured for the third case whereby the rGO treated side faces the membrane (about 4% higher peak power density than using untreated CP electrodes). These results are summarized in Table II.

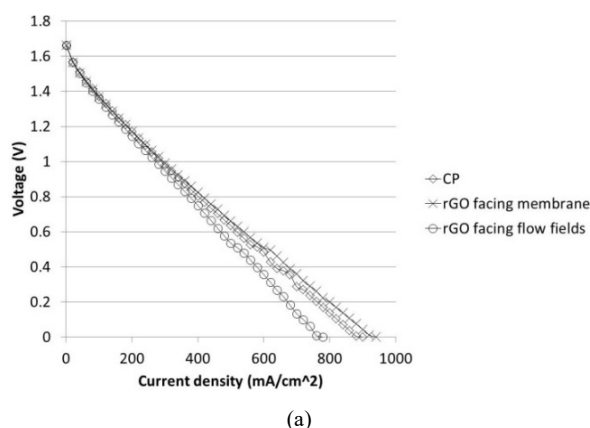
It is envisaged that higher peak power densities could be obtained if the VRFB was allowed to discharge from 100% SOC to much lower values. However, such a power density is not always beneficial as the overpotentials associated with them result in lower voltage efficiencies [5]. Thus, maintaining the same SOC and measuring a peak power density may be more favorable [1].

### IV. CHARGE AND DISCHARGE

Finally charge/discharge experiments were carried out using equal volumes of electrolytes for both half-cells. For the rGO deposited samples (single-sided only were used), the deposition side was facing the membrane and not the flow fields in all respective cases. Fig. 4 shows the profiles for a VRFB with just normal CPs against those for the system having rGO deposited CPs. The figures of merit (the utilization, current efficiencies and energy efficiencies) are shown in Table III. It is clear from Fig. 4 that rGO treated electrodes resulted in better performance for the VRFB.

TABLE II  
KEY PERFORMANCE METRICS WITH DIFFERENT CP ELECTRODES  
(UNTREATED AND RGO MODIFIED SAMPLES)

Sample	Area specific resistance ( $m\Omega cm^2$ )	Peak power density ( $mW/cm^2$ )
Untreated CP	955	323
rGO deposited sample facing flow fields	1045	301
rGO deposited sample facing membrane	940	335



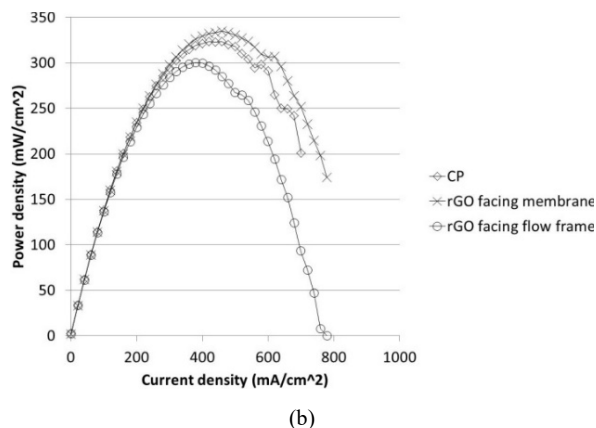


Fig. 3 (a) Polarization and (b) power density curves for three CP samples (untreated CP, rGO deposited sample facing flow fields and rGO deposited sample facing the membrane) in an operational VRFB

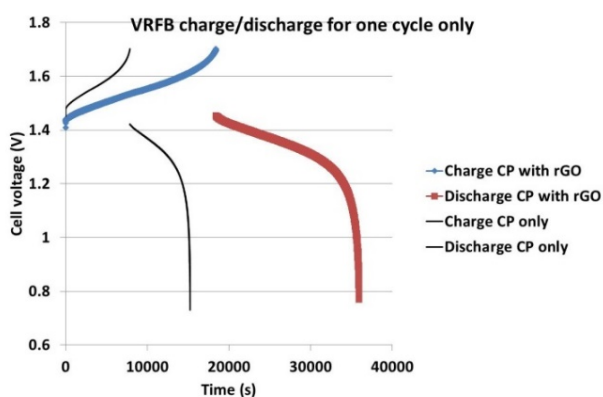


Fig. 4 Charge and discharge performance of a VRFB after one cycle for both untreated and rGO deposited CP electrodes

Fig. 5 shows the VRFB charge/discharge behavior after 10 cycles. Even here rGO shows far better performance than pristine CP electrodes. The figures of merit for this graph are also provided in Table III.

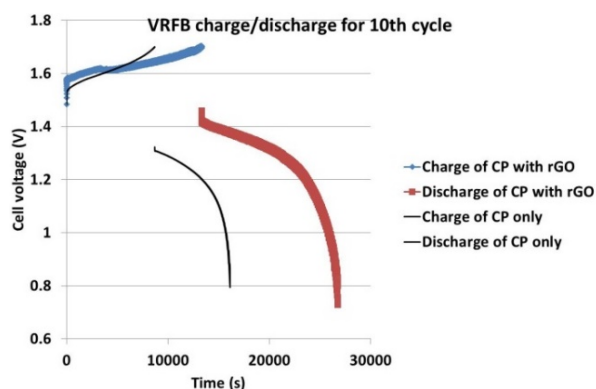


Fig. 5 Charge and discharge performance of a VRFB after ten cycles for both untreated and rGO deposited CP electrodes

The behavior of the VRFB after undergoing 20 continuous cycles is shown in Fig. 6. The rGO modified CP electrodes

performed far better than the pristine CP samples as is also illustrated by the figures of merit in Table III.

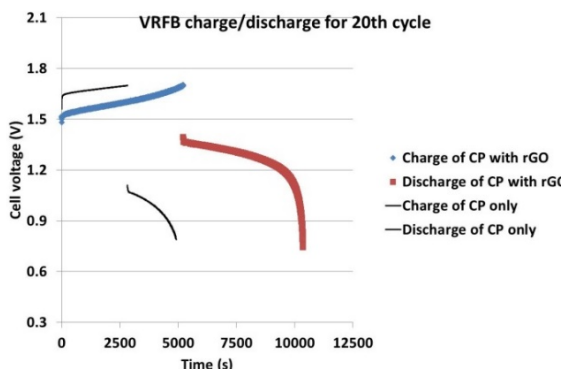


Fig. 6 Charge and discharge performance of a VRFB after twenty cycles for both untreated and rGO deposited CP electrodes

TABLE III  
FIGURES OF MERIT FOR A VRFB OPERATING WITH AND WITHOUT RGO COATING OF CP ELECTRODES

Cycle	Utilization (%)	Current efficiency (%)	Energy efficiency (%)
Pristine CP			
1	93.64	87.93	73.06
10	85.45	73.27	54.59
20	73.86	54.41	32.02
CP with rGO			
1	95.02	90.55	77.32
10	100.00	100.00	79.49
20	98.35	96.95	76.88

It is clearly seen from Table III that the pristine CP deteriorates in performance with cycling as efficiencies of the VRFB drops dramatically. In contrast, rGO coated CP electrodes do not show any such signs of deterioration. It is unclear as to why the efficiencies increased by the end of the 10<sup>th</sup> cycle, but they were fairly similar to the first cycle by the 20<sup>th</sup> run. It is possible that some water may have evaporated from the electrolytes due to continuous bubbling of nitrogen and the concentrations of active species had increased. Some water was added to the anolyte to compensate for this evaporation by the end of the 10<sup>th</sup> cycle (this probably meant that the results shown for the 20<sup>th</sup> run were for electrolytes having lower vanadium concentration than that for the 10<sup>th</sup> run). Therefore, future work is envisaged whereby the nitrogen would be humidified to minimize water evaporation.

It is also noted that there was no leaching of rGO that was deposited on the CP samples. This indicated that the deposits were not only stable on the CP electrodes but also enhanced the durability of the CP in highly acidic conditions (5 M sulfuric acid).

## V. CONCLUSION

rGO was successfully used to modify CP electrodes by means of EPD. Only a single-sided deposit was used as earlier work showed that double-sided deposition did not improve charge transfer kinetics of the  $\text{VO}_2^+/\text{VO}_2^+$  couple. About 4%

higher peak power density was obtained when the rGO was facing the Nafion membrane in comparison to the untreated CP. For the case when the rGO was facing the flow fields, the peak power density was lower by 7% in comparison to the untreated CP. In addition, the VRFB efficiencies were much better for rGO modified CP electrodes in comparison to the pristine CP samples. This was especially evident from cycling tests.

*Phys. Chem. B*, vol. 117, no. 6, pp. 1502-1515, 2013.

#### ACKNOWLEDGMENT

The authors are grateful for the funding provided by the EPSRC project EP/L014289/1.

#### REFERENCES

- [1] V. Yufit, B. Hale, M. Matian, P. Mazur, and N. P. Brandon, "Development of a regenerative hydrogen-vanadium fuel cell for energy storage applications," *J. Electrochem. Soc.*, vol. 160, no. 6, pp. A856-A861, March 2013.
- [2] C. L. Chen, H. K. Yeoh, and M. H. Chakrabarti, "One Dimensional Mathematical Modelling of the All-Vanadium and Vanadium/Oxygen Redox Flow Batteries," *ECS Trans.*, vol. 66, no. 10, pp. 1-23, 2015.
- [3] M. H. Chakrabarti, N. P. Brandon, S. A. Hajimolana, F. Tariq, V. Yufit, M. A. Hashim, M. A. Hussain, C. T. J. Low, and P. V. Aravind, "Application of carbon materials in redox flow batteries," *J. Power Sources*, vol. 253, pp. 150-166, May 2014.
- [4] D. Aaron, Z. Tang, A. B. Papandrew, and T. A. Zawodzinski, "Polarization curve analysis of all-vanadium redox flow batteries," *J. Appl. Electrochem.*, vol. 41, pp. 1175-1182, Oct. 2011.
- [5] D. S. Aaron, Q. Liu, Z. Tang, G. M. Grim, A. B. Papandrew, A. Turhan, T. A. Zawodzinski, and M. M. Mench, "Dramatic performance gains in vanadium redox flow batteries through modified cell architecture," *J. Power Sources*, vol. 206, pp. 450-453, May 2012.
- [6] Q. Zheng, F. Xing, X. Li, T. Liu, Q. Lai, G. Ning, and H. Zhang, "Investigation on the performance evaluation method of flow batteries," *J. Power Sources*, vol. 266, pp. 145-149, Nov. 2014.
- [7] Q. H. Liu, G. M. Grim, A. B. Papandrew, A. Turhan, T. A. Zawodzinski, and M. M. Mench, "High Performance Vanadium Redox Flow Batteries with Optimized Electrode Configuration and Membrane Selection," *J. Electrochem. Soc.*, vol. 159, no. 8, pp. A1246-A1252, July 2012.
- [8] M. P. Manahan, Q. H. Liu, M. L. Gross, and M. M. Mench, "Carbon nanoporous layer for reaction location management and performance enhancement in all-vanadium redox flow batteries," *J. Power Sources*, vol. 222, pp. 498-502, Jan. 2013.
- [9] P. Han, Y. Yue, Z. Liu, W. Xu, L. Zhang, H. Xu, S. Dong, and G. Cui, "Graphene oxide nanosheets/multi-walled carbon nanotubes hybrid as an excellent electrocatalytic material towards  $\text{VO}_2^+/\text{VO}^{2+}$  redox couples for vanadium redox flow batteries," *Energy Environ. Sci.*, vol. 4, no. 11, pp. 4710-4717, 2011.
- [10] M. H. Chakrabarti, C. T. J. Low, N. P. Brandon, V. Yufit, M. A. Hashim, M. F. Irfan, J. Akhtar, E. Ruiz-Trejo, and M. A. Hussain, "Progress in the electrochemical modification of graphene-based materials and their applications," *Electrochim. Acta*, vol. 107, pp. 425-440, Sept. 2013.
- [11] B. Chakrabarti, D. Nir, V. Yufit, F. Tariq, J. Rubio-Garcia, R. Maher, A. Kucernak, P. V. Aravind, and N. Brandon, "Performance Enhancement of Reduced Graphene Oxide-Modified Carbon Electrodes for Vanadium Redox-Flow Systems," *ChemElectroChem*, vol. 4, pp. 194-200, 2017.
- [12] Q. Xu, T. S. Zhao, and C. Zhang, "Performance of a vanadium redox flow battery with and without flow fields," *Electrochim. Acta*, vol. 142, pp. 61-67, Oct. 2014.
- [13] W. Chartarrayawadee, S. E. Moulton, D. Li, C. O. Too, and G. G. Wallace, "Novel composite graphene/platinum electro-catalytic electrodes prepared by electrophoretic deposition from colloidal solutions," *Electrochim. Acta*, vol. 60, pp. 213-223, Jan. 2012.
- [14] A. Di Blasi, N. Briguglio, O. Di Blasi, and V. Antonucci, "Charge-discharge performance of carbon fiber-based electrodes in single cell and short stack for vanadium redox flow battery," *Appl. Energy*, vol. 125, pp. 114-122, July 2014.
- [15] A. Chavez-Valdez, M. S. P. Shaffer, and A. R. Boccacini, "Applications of Graphene Electrophoretic Deposition. A Review," *J.*